

Original article

Methods and application for photorealistic rendering and lighting of ancient buildings

Maurizio Rossi ^{a,*}, Daniele Marini ^b, Alessandro Rizzi ^c

^a *Dip. Industrial Design Art & Communication, Politecnico di Milano, Via Durando, 38/A, 20158 Milano Italy*

^b *Dip. Informatica e Comunicazione, Università di Milano, Via Comelico, 39, 20135 Milano Italy*

^c *Dip. Tecnologie dell'Informazione, Università di Milano (Polo di Crema), Via Bramante, 65, 26013 Crema Italy*

Received 10 June 2003; accepted 1 December 2003

Abstract

Within the field of cultural heritage restoration, experts are interested in the visual analysis of data describing status and history of ancient monuments. The use of computers together with image synthesis techniques can support the visual analysis and comparison of restoration simulation. The results of these computations are usually distributed over many sites that can be viewed by VRML and Java technology, which are well-suited for describing and visualizing geometrical models and data interaction over the Internet. Unfortunately, the poor quality of VRML real time rendering is a bottleneck for any analysis based on accurate image synthesis methods. Another problem in reproducing images with photorealistic rendering derives from the adaptation mechanisms of the human visual system. We describe a method and its implementation for providing high quality photorealistic image synthesis of ancient building materials, considering also a final adaptation stage able to simulate the lighting and color adaptation phases of a human observer. In this method, a network based Java application manages geometric 3D models of ancient buildings to provide an editing interface and to manage high quality photorealistic snapshots. Simple 3D VRML data are enhanced with radiometric data derived by gathering measurements on the actual material taken from the site to reproduce. In the example presented in this paper, we have used measurements taken from the ancient Roman Aosta Theatre. A server-based optimized rendering application computes photorealistic images on radiometric data, that are subsequently applied as input to an algorithm simulating the human visual system perception. This latter phase is able to emulate the human local lightness, and chromatic adaptation mechanisms. The enhanced interaction with high quality images of the model through the Java application, allows a visual qualitative evaluation of restoration hypotheses. It also provides a tool that is able to show the final appearance of the model under assigned lighting conditions, as observed by a human being “inside” the virtual environment.

© 2004 Elsevier SAS. All rights reserved.

Keywords: Photorealistic rendering; Lighting; Visual appearance; Color processing; Chromatic adaptation; Restoration simulation

1. Research aims

A novel field of application of image synthesis deals with computer restoration simulation of ancient buildings. Multimedia techniques supported on local disk or based on networked hypermedia via the Internet provides methods to convey complex information in the field of cultural heritage to experts and non-experts through visual representation and visual interaction. While cultural heritage experts may be interested in using computer methods to explore hypothetical

alternatives in order to select optimum techniques for restoring and preserving monuments, non-experts are usually interested in general information about all historical and artistic notes that may increase a deeper appreciation and understanding of cultural heritage sites.

In this paper we focus on image synthesis quality enhancement to provide experts a powerful tool enabling, through visual representation, qualitative evaluation of materials surface modification of ancient buildings. We suggest that this methodology may be useful to explore hypothetical restoration alternatives in order to provide essential information on techniques for restoring and preserving monuments.

The research field of image synthesis, starting in the early '80, focused primarily on image–time optimization, and only

* Corresponding author.

E-mail addresses: maurizio.rossi@polimi.it (M. Rossi), daniele.marini@unimi.it (D. Marini), rizzi@dti.unimi.it (A. Rizzi).

recently turned its attention to the problem of accurate material reflectance and illumination condition reproduction. The available image synthesis systems are able to compute color-precise images without considering the light distortion associated with the physical acquiring conditions.

In Fig. 1, we present an image synthesis pipeline that takes into account a photorealistic representation of the real world, depicting four different stages in which extensive research has been done.

Commercial and public domain rendering systems do not take into account radiometric properties of light but directly compute the lighting models in the colorimetric field, describing the materials with *RGB* colorimetric triplets. In our opinion, this approach may be useful only for fast image production purposes. Our assumption is based on the hypothesis that it is incorrect to describe a complex phenomenon such as light–materials interaction in terms of values (*RGB*) that are the results of the tristimulus acquisition process. In fact, the tristimulus theory cannot cope with metamerism, color constancy or other typical perceptive phenomena.

The result produced by computing the illumination model should be a spectral radiance function of wavelength $L_e(\lambda)$. This may be reduced to the CIE *XYZ* absolute values, described by the tristimulus theory [1], only in the final stage with the following integrations :

$$X = K_{\max} \int_{380}^{780} L_e(\lambda) \bar{x}(\lambda) d\lambda$$

$$Y = K_{\max} \int_{380}^{780} L_e(\lambda) \bar{y}(\lambda) d\lambda$$

$$Z = K_{\max} \int_{380}^{780} L_e(\lambda) \bar{z}(\lambda) d\lambda$$

where $K_{\max} = 683 \text{ lm/W}$ is the maximum value of the human photopic luminous efficacy function [1]. The *XYZ* absolute color triplets then must be transformed to the display relative *RGB* color space [2] with the following linear transformation :

$$\begin{bmatrix} R \\ G \\ B \end{bmatrix} = M^{-1} \cdot \begin{bmatrix} X \\ Y \\ Z \end{bmatrix}$$

where M is the matrix of CIE *XYZ* tristimulus values of the three *R*, *G* and *B* phosphors of the monitor. All these steps are represented in Fig. 2. Unfortunately the CIE tristimulus approach does not take into account adaptation phenomena of the human visual perception. So an image produced only with the above described steps cannot take into account adaptation mechanisms that the human vision system uses to produce a stable reality perception [3,4], producing beautiful but unreal images.

An interesting feature, in the restoration support field, is the capability to generate images of restoration hypothesis that have to appear as real restorations. The term “appear” understates various problems of visual match and photorealism. These effects have to be added in the photorealistic image generation pipeline to augment the naturalness of an image.

To explore the feasibility and effectiveness of this approach, a test has been done on data describing the ancient Roman theatre of Aosta in northern Italy [5,6]. This is quite a rare example of a covered Roman theatre because its geographical position are under very inhospitable climatic conditions which include cold temperatures and significant amounts of moisture for several months during the year. For this reasons its constituent materials, consisting of travertine ashlar and pudding stones are strongly degraded and only the front and the foundation have survived (see Fig. 3).

Information about this theatre includes geometric data, images and descriptive information collected by the cultural heritage experts. These descriptive and pictorial data have been used to further improve the degree of detail and accuracy of the ancient building description and representation. In particular, architectural properties have been extracted by reconstructing 3D models of stones from digital camera acquisition [7] and then CAD refinement, as shown in Fig. 4. Spectral properties of ancient construction materials have been measured in laboratory under reconstructive conditions (that is after cutting and/or polishing the samples, bringing them to their original conditions or after a cleaning process on site).

A 3D reconstruction of the whole theatre front has been carried out to create a VRML model for accessing the col-

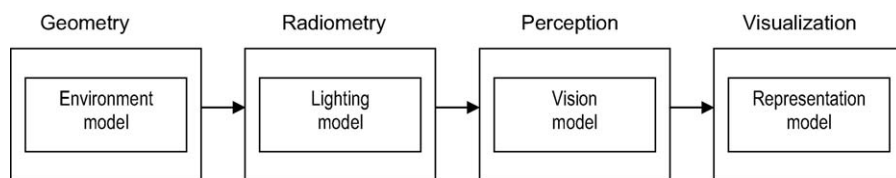


Fig. 1. Image synthesis production flow.

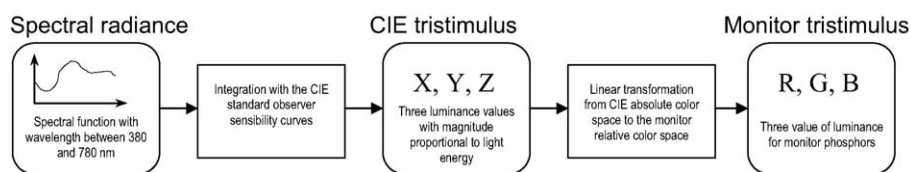


Fig. 2. From light signal radiance to light reproduction on the monitor.

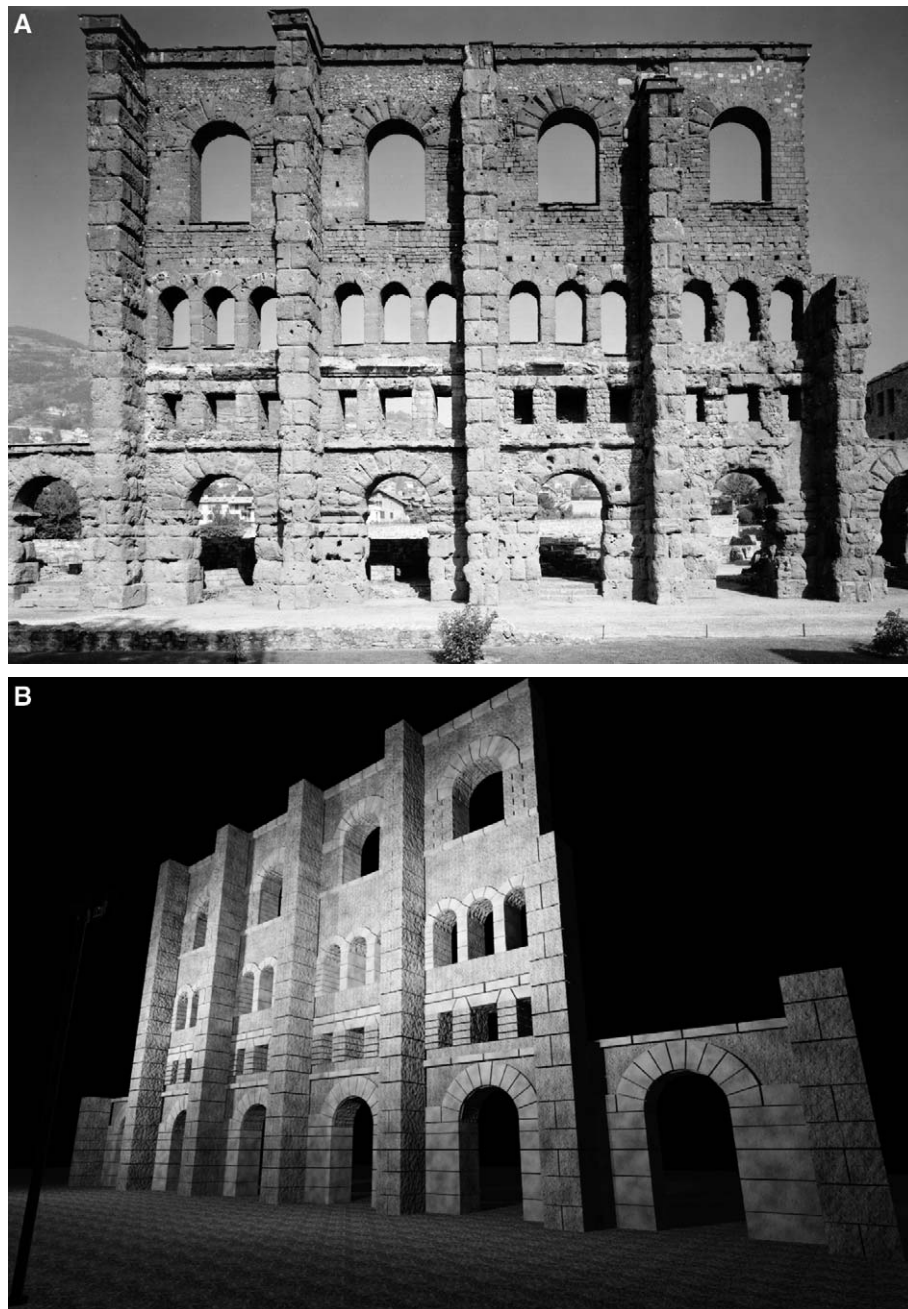


Fig. 3. The survived front of theatre : (a) photographic image (b) photorealistic rendering under known lighting condition.

lected information using Web browsers. Advanced graphics rendering is necessary for using the system as a virtual restoration test bed. This is done exploring the effects of conservation simulation, or restoration hypothesis, and attempting to capture the architectural essence of the original building under assigned lighting condition. Experts may use the link between photorealistic rendering, optical and physical properties of materials to better control conservation and restoration processes. Adding a chromatic post-filtering on the spectral data, not only helps to render a more realistic image, but also helps in avoiding metameric ambiguities in the light–matter interaction.

2. Experiments

2.1. The radiometric rendering

The critical problem in realistic rendering of complex models, such as ancient buildings, is to control their visual appearance. One possible way of accomplishing this is the adoption of texture mapping methods to realize an “impressionistic” rendering. This is an efficient solution for a system with specific hardware architectures, supporting real time navigation through textured surfaces, but it can give only a rough idea of their real aspect. In order to increase the degree

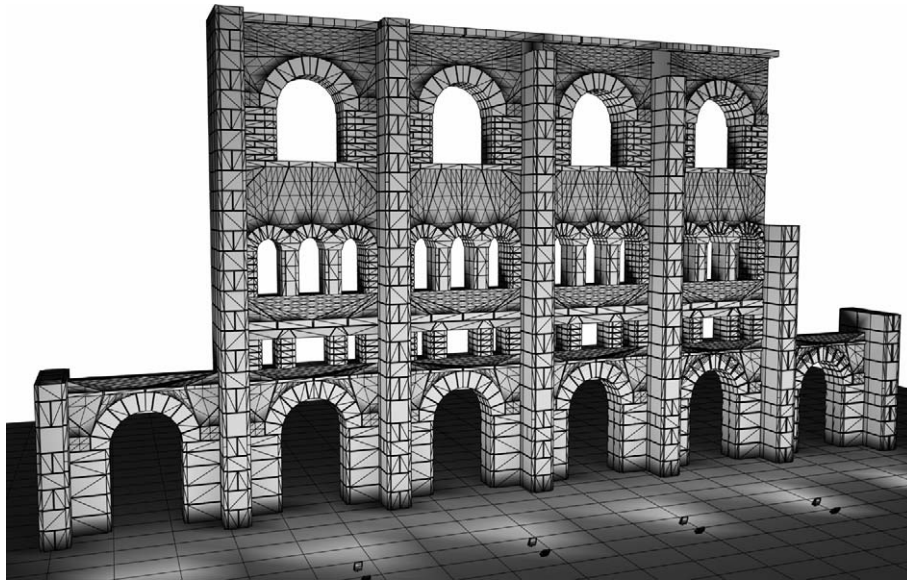


Fig. 4. The survived front of theatre : CAD refinement of the geometrical structure.

of accuracy, it is necessary to use photorealistic methods based on physically accurate lighting model. In our test, advanced ray tracing [8] has been adopted as a global illumination model and a modified Cook and Torrance [9,10] as a local illumination model. With this method it is impossible to realize a real time rendering, but the results are of great interest, since a link between structural and chemical characteristic of the samples is maintained in order to render their visual appearance. Using ray tracing as a global illumination model leads to a well-known error in underestimating the mutual diffuse inter-reflection of light from objects of the scene. Nevertheless, this error in computing the illumination of an external building is lower than in an internal ambient for which the radiosity [9] method is more accurate. The choice of the Cook–Torrance local illumination model has been suggested by its radiometric properties and by the physically accurate description of light behavior in its interaction with surface materials. Moreover, we extended the original formula to include definition of light sources according to the lighting industry standards [11].

To better understand this approach, we recall how the light–material interaction is simulated with the chosen rendering system. Commercial rendering programs adopt an approximate illumination model to compute colors shading, following an implementation of the tristimulus theory, defining colors in terms of *RGB* triplets. On the contrary, in our advanced rendering system, based on a radiometric illumination model, the reflected radiance is computed for spectral intervals between 380 and 780 nm with 5 nm steps, allowing us to compute the reflected radiance $L_{e,R}(\lambda)$ in terms of the incident irradiance $E_e(\lambda)$ and the bi-directional reflectance (BRDF) $\rho(\lambda)$:

$$L_{e,R}(\lambda) = \rho(\lambda) \cdot E_e(\lambda) \quad (1)$$

where $\rho(\lambda)$ is approximated as described by Cook and Torrance [9]. The incident spectral irradiance on the sampled

surface point is computed using the ray tracing global illumination model as the sum of spectral irradiance coming from the luminaries and the spectral irradiance coming from other bodies through specular reflection.

Working in cooperation with Istituto per le Tecnologie Applicate ai Beni Culturali Consiglio Nazionale delle Ricerche, Roma (ITABC-CNR) we collected data for this case study. The geometric survey and the reconstruction have been made by a professional CAD refinement study on the whole building face (Fig. 4) and on single sample stones (Fig. 5). These 3D data were converted to VRML models and photos of the actual materials were digitally acquired and applied as textures to the geometrical model [12,13] to get an impressionistic representation of the building. In addition, much descriptive information has been collected from a visual inspection made by cultural heritage experts [14,15] consisting of a large quantity of manuscript information, photos, charts and images, and has been linked to the 3D VRML model of the building.

A high resolution geometric reconstruction of the 3D models of some sample stones has been done with digital camera multiple acquisitions [16] (Fig. 5). This geometrical data was also converted in VRML and textured. Finally these data has been included in the whole model as another structure with different level of detail.

2.2. Material characterization

To apply the photorealistic lighting model described above in Eq. (1) we need to describe materials using spectral reflectance instead of *RGB* color. Following this assumption we performed a spectrometric analysis of pudding stones and travertine ashlars samples that resulted in spectral hemispherical reflectivity curves. These analyses have been conducted on samples in their natural state of degradation, as well as after cutting and polishing, to get reflectivity curves

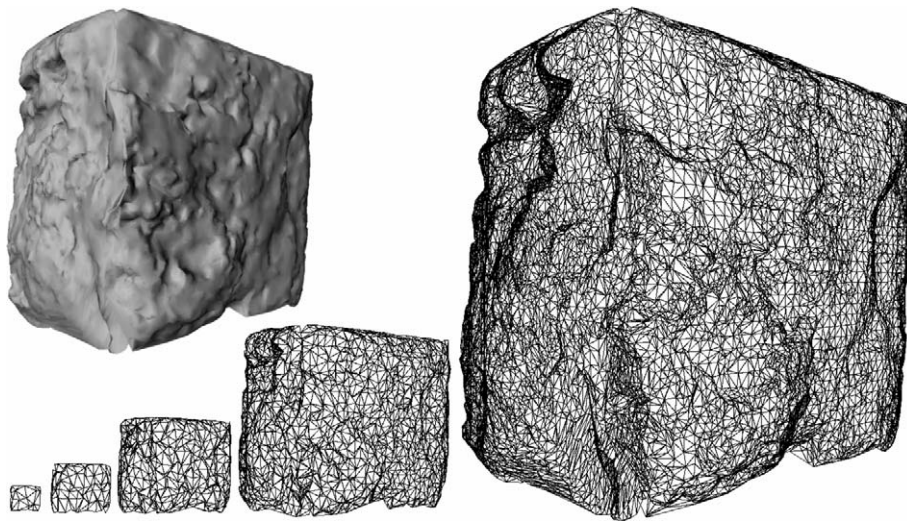


Fig. 5. Single stone at different detail levels, wire frame and shaded.

under different conditions, simulating in this way the effects of restoration of a cleaning process. We measured the hemispherical reflectivity as a function of light wavelength in the range of visible spectrum, from 380 to 780 nm. All measured samples were taken from the stone’s surface, pulverized to fit into a Beckmann reflectance spectrophotometer with a magnesium oxide coated integrating sphere.

Fig. 6 reports the hemispherical reflectance of a travertine–ashlars in a dirty degraded sample, and after cutting and polishing it. The dirty surface has little differences in the spectral response, but reflects less light than the cleaned one. Fig. 7 reports the hemispherical reflectance of a pudding stone sample in both degraded and polished condition. The difference in the two cleaned stone reflectances is due to the granular nature of pudding stone that is a compound of different minerals, while the dirty sample does not show these differences.

Considering only the hemispherical reflectance $\rho_e(\lambda)$ instead of the complete bi-directional reflectance distribution

function $\rho(\lambda)$ results in a small error in Eq. (1) because travertine–ashlars and pudding stones have a very diffuse reflectance properties, similar to the lambertian one.

2.3. The lighting computation

The second key point in the lighting model used in the radiometric rendering is in the light source definition. We decided to describe the light source adhering to luminaries standard as defined by lighting industry. Usually spectral properties are defined by the spectral relative power distribution S_e , which is a function of wavelength λ :

$$S_e(\lambda) = 100 \cdot M_e(\lambda) / M_e(555) \tag{2}$$

for $380 \leq \lambda \leq 780$ nm, where $M_e(\lambda)$ is the spectral radiant exit of the light source. The 555 nm wavelength value is used to normalize because in this point the human luminous efficacy function has its maximum value. The luminaries intensity distribution is defined by the photo goniometric diagram

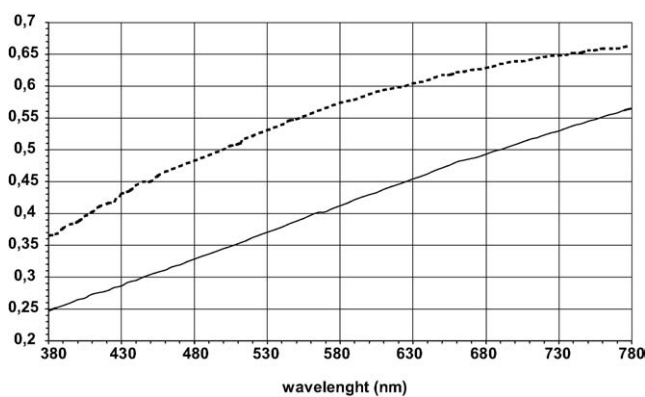


Fig. 6. Hemispherical reflectance of a travertine–ashlars sample : the solid line represent a dirty degraded sample while the dashed line represents a cut and cleaned one.

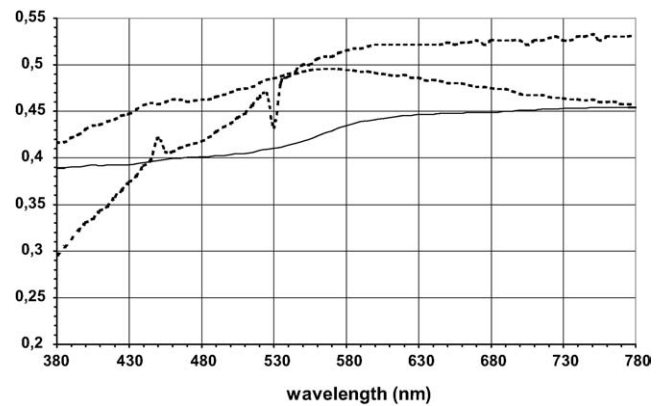


Fig. 7. Hemispherical reflectance of a pudding stone sample, the solid line represents a dirty degraded sample while the two dashed line represent cut and cleaned one taken from two different surface positions.

$I_v(\theta^0, \phi^0)$ that defines light intensity distribution (LID, measured in candles) in all directions around the light source with respect to a reference position and orientation [11].

The problem arising when using luminaries standard definition in the relation Eq. (1) as light irradiance is in the different dimension of the computed factors, indeed $E_e(\lambda)$ is a radiometric function of wavelength, while the standard defines $I_v(\theta^0, \phi^0)$ which is the total photometric luminous intensity that is a function of the direction with respect to the reference axis of the light source. We would obtain the incident spectral irradiance coming from the light source. In our method we suppose that the spectral relative power distribution $S_e(\lambda)$ is known. This is a function generally available from lighting industry and CIE international standards [17,18]. Ray tracing is the global illumination model, thus light coming from luminaries is sampled with rays of assigned direction and in the computation of the contribution of a single ray we can ignore the luminous intensity dependence from direction and consider it as a single assigned total value I_v .

As a first step, we recall the following fundamental radiometric and photometric relations [2,19] :

$$E_e(\lambda) = \cos\alpha \cdot I_e(\lambda) / r^2 \tag{3}$$

$$I_v = \int_{380}^{780} I_v(\lambda) d\lambda \tag{4}$$

$$I_v(\lambda) = K(\lambda) \cdot I_e(\lambda) ; E_e(\lambda) = K(\lambda) \cdot E_e(\lambda) \tag{5}$$

$$M_e(\lambda) = \frac{d\Phi_e(\lambda)}{dA} ; I_e(\lambda) = \frac{d\Phi_e(\lambda)}{d\omega} \tag{6}$$

The Eq. (3) shows the relation between the spectral irradiance $E_e(\lambda)$ falling on a surface irradiated by a source which emits a spectral radiant intensity $I_e(\lambda)$ at a distance r ; and coming with a α angle with respect to the normal surface. This is the fundamental relation to determine the spectral irradiance on a sampled point due to a light source. We do not know the value of the spectral radiant intensity $I_e(\lambda)$ emitted from the luminaries but only I_v and $M_e(\lambda)$. The Eq. (4) computes total values from the spectral functions. The Eq. (5) shows the relation between radiometric (I_e) and photometric (I_v) functions, weighted by the human spectral luminous efficacy $K(\lambda)$ [1]. The Eq. (6) are the radiometric definitions of the radiant exit and the radiant intensity, respectively, as functions of the radiant flux $\Phi_e(\lambda)$, the area A and the solid angle ω .

Using Eqs. (5) and (6) we could rewrite relation Eq. (2) in the following way :

$$S_e(\lambda) = 100 \cdot \frac{I_e(\lambda)}{I_e(555)} = 100 \cdot \frac{I_v(\lambda)}{I_v} \cdot \frac{K(555)}{K(\lambda)}$$

and if we set

$$C = \frac{I_v(555)}{100 \cdot K(555)}$$

then we compute the spectral photometric light intensity in the following way :

$$I_v(\lambda) = \frac{I_v(555)}{100 \cdot K(555)} \cdot K(\lambda) \cdot S_e(\lambda) = C \cdot K(\lambda) \cdot S_e(\lambda) \tag{7}$$

The value $I_v(555)$ is unknown, thus, to determine the value of the constant C , from the relation Eq. (4) we could write :

$$I_v = \int_{380}^{780} C \cdot K(\lambda) \cdot S_e(\lambda) d\lambda$$

thus,

$$C = I_v / \int_{380}^{780} K(\lambda) \cdot S_e(\lambda) d\lambda$$

Substituting this expression for C in the Eq. (7) we obtain the spectral luminous intensity function $I_v(\lambda)$ and using the Eq. (5) we could finally compute the value of the spectral irradiance $E_e(\lambda)$:

$$E_e(\lambda) = \frac{I_v \cdot S_e(\lambda)}{r^2 \cdot \int_{380}^{780} K(\lambda) \cdot S_e(\lambda) \cdot d\lambda} \cdot \cos\alpha \tag{8}$$

The Eq. (8) computes the incident spectral irradiance function $E_e(\lambda)$ on a sampled point of a surface, due to a light source at distance r ; along a ray with angle α (with respect to the surface normal), with a spectral distribution $S_e(\lambda)$ and with total luminous intensity I_v in the sampled direction.

Natural lighting from the sun is defined by a source, which has light rays coming from an infinite distance, every ray parallel to each other in a defined direction. This light model is defined by the total illuminance (in lux) $E_{v,0^\circ}$ measured on a surface orthogonal to the considered direction. Experimental measurement acquired using a luxmeter are shown in Table 1.

2.4. The experimental tool

To manage objects and light sources, we developed a prototypal Java interface to enhance the limited VRML material and light source description capabilities [20]. This application is the core tool for the management of the data described above. Since the VRML browser does not allow the user to interactively modify the data, this Java application assists the expert operator in accessing local or remote VRML geometrical models of the cultural heritage building,

Table 1
Direct sun illuminance

$E_{v,0^\circ}$ (lux)	Source
100 000	Light from the sun 50° over the horizon
10 000	Light from the sun in a cloudy day
0,2	Light in night with full moon

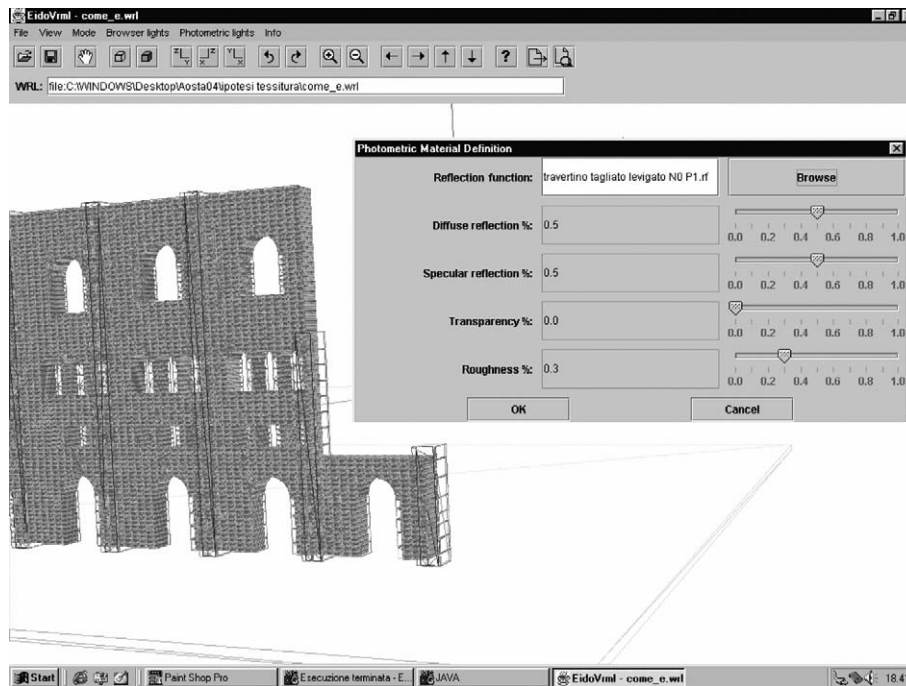


Fig. 8. The Java interface program. This application provides a tool to manage the 3D data of the cultural heritage building associating spectral reflectance data to materials constituting the building. It also defines photometric light sources and prepares data for the photorealistic rendering phase.

associating the spectral properties of the material and photometric light definition to the model (Fig. 8).

This application, based on the Java and Java3D technology from Sun Microsystems, can be executed on different operating systems. This programming language provides tools for accessing and managing 3D virtual reality models and remote Internet data. In fact, Java3D is based in the OpenGL graphics library, on systems with dedicated hardware support, the display performance of the geometrical data could be quite effective even for very complex models. Moreover, an important benefit of the application interface is the capability of managing local and remote data assuming URLs as the basis for locating different types of data resources. In the field of cultural heritage management, this is a key feature since it could not exist a unique main database and data are usually recorded in a variety of different sites. Any kind of data could be linked and inspected to/from the model of the building simply with the support of an external Internet browser.

VRML does not provide the definition of materials based on a spectral basis but only on a classic colorimetric definition. Another obvious limitation of this standard is in the quality of the images rendered and produced with VRML browsers. To guarantee a virtual reality interaction and a fast animation, the browser rendering is based on simple shading techniques without any regard to global illumination effects and accurate light–material interaction. Spectral data are simply ignored by VRML browsers. Nevertheless, these data plays a fundamental role when the user starts the photorealistic snapshot. The activation of the photorealistic rendering program is accomplished through a simple system call as a separate process, written in C language which has been

reported to different architectures. The interface allows to associate reflectance spectra, such as those defined in Figs. 6,7, with object models. Thus restoration expert may simulate any kind of material appearance based on the original constituting situation and on the actual state of degradation, exploring hypothesis of restoration and conservation.

Therefore, in the application interface, an interactive navigation is implemented using impressionistic rendering with textured images, while accurate rendering is used for single viewpoint displays. The expert user can interactively choose to generate the rendering of a particular element or of the entire building from a desired viewpoint, testing the results of a “virtual” restoration.

In conclusion, the Java interface is not simply a modeling system or a VRML browser, but an experimental interactive tool with extended features for the management of photorealistic data.

In Fig. 9, the interface application manages a high resolution model of a travertine–ashlars block inserted as detailed geometrical level in the VRML model of the Aosta Roman Theatre. The particular is then visible both degraded and virtually polished through photorealistic rendering. These images have been generated giving the reflectance of each surface material condition and a white light source which spectral composition is the CIE D65 standard illuminant.

2.5. The filtering for visual appearance

In the computation of a highly detailed view, the appearance is preserved from a photometric point of view, but not from a human observer’s viewpoint. To better realize the final visual appearance we propose to post-filter the synthetic

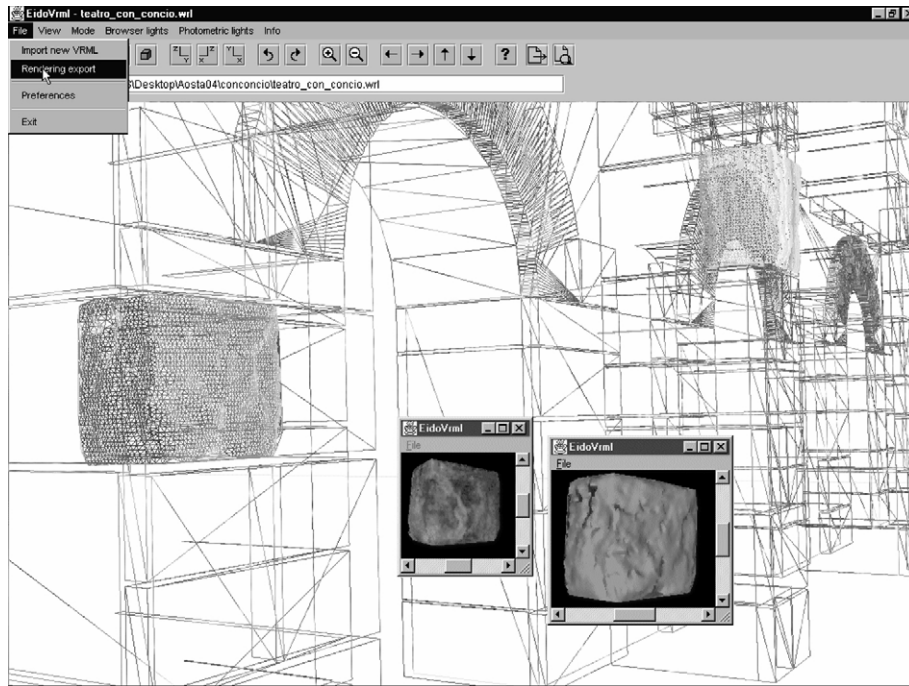


Fig. 9. The Java interface that managing the photorealistic rendering of a travertine-ashlars block. The two small windows show two different renderings with simulation of two different level of surface material situation. Smallestest window : a degraded material. Bigger window : an ideally polished material.

images with the Retinex algorithm, which is able to simulate some of the adaptation mechanism of the human vision system [3].

We recall a mathematical treatment of the algorithm proposed by Land and McCann [21], from which our algorithm derives [3,4,22]. The basic principle is that our vision system forms the final appearance of a point in the scene, a pixel in the digital image, “computing” the relative luminance appearance, called *lightness*, separately in the three cone channels *l*, *m*, *s*, roughly corresponding to *RGB* in the field of digital imaging.

The average lightness at the pixel *i* of the input image produced by the Retinex filter, is the mean value of the relative lightnesses, computed over a number *N* of random paths through the image, ending at the pixel (Fig. 10), separately for each chromatic channel.

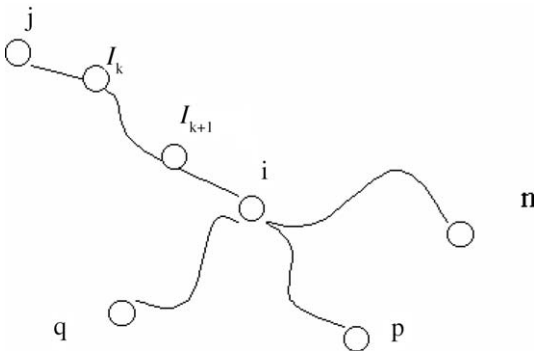


Fig. 10. Computation of the average relative reflectance.

The lightness at the end of each path is computed as a ratio between the channel intensities *I* of the path pixels, in the following way :

$$L_{l,m,s}^{i,j} = \sum_{k \in \text{path}} \delta \log \frac{I_{k+1}}{I_k}$$

and :

$$\delta = \begin{cases} 1, & \text{if } \left| \log \frac{I_{k+1}}{I_k} \right| > \text{threshold} \\ 0 & \text{else} \end{cases}$$

where *I_k* and *I_{k+1}* are, respectively, the channel intensities at points *k* and *k+1* along the random paths (Fig. 10). These computations are executed independently for the three *RGB* chromatic channels.

The above model depends on many parameters [23,24]. The randomness and the number of paths that are chosen for the computation of the relative lightness are critical for speed and accuracy of the result. Mimicking the receptive fields distribution of cortical area V4 [25], we have implemented a Brownian motion approximation to generate the random paths (Fig. 11) along which the ratio computations are made [3]. The threshold plays the role of discounting non-uniform illumination, since it makes unessential low-reflectance ratios. Moreover, during a path computation, Retinex has a mechanism so that if a brighter area is found, the cumulated relative lightness is reset; this forces the computation to restart from the brightest areas. In other words, the effect of

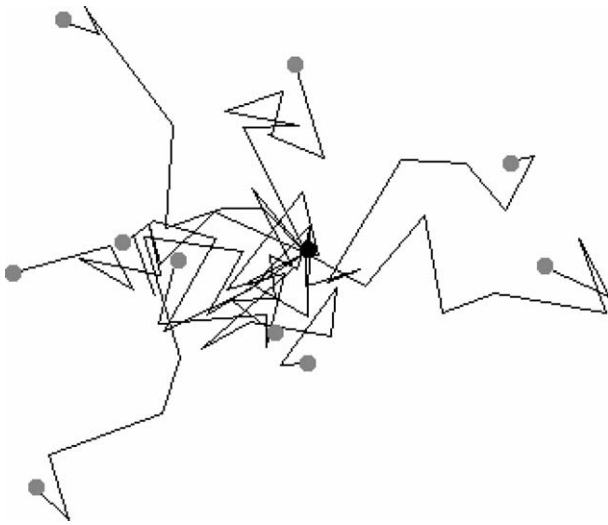


Fig. 11. Example of 10 Brownian paths.

the reset mechanism is to consider the brightest area of an image as the reference value of the color white.

The Retinex algorithm can be effectively used to equalize colors or to simulate chromatic illusion [22]. In order to test the effectiveness of this solution, we have generated different synthetic images under various CIE standard illuminants: A, B, C, and D65. Comparisons between images in color Fig. 12 shows differences in images with and without Retinex post-filtering. As for human color perception the post-filtering compensates for chromatics dominant produced by a CIE “B” light which has a warm dominant. On the contrary, post-filtering does not affect the sample illuminated by the CIE “D65” light which is an ideal example of “white light”.

3. Conclusions

In this paper a tool for visual analysis and comparison of restoration simulation via the Internet has been presented. It has been devised to overcome the poor quality of VRML real time rendering, providing high quality photorealistic image synthesis of ancient building materials, also considering a final adaptation stage able to simulate the lighting and color adaptation phases of a human observer. The enhanced interaction with high quality images of the model through the Java application, allows a visual qualitative evaluation of restoration hypotheses. It also provides a tool that is able to show the final appearance of the model under assigned lighting conditions, as observed by a human being “inside” the virtual environment.

In the example presented in this paper, we have used measurements taken from the ancient Roman Aosta Theatre. The results of virtual restoration (based mainly in this case study on cleaning and/or polishing the stones) can be displayed on single samples or applied to the entire building.

This process computes the (R, G, B) values from the spectral radiance $L_c(\lambda)$ and then post-filter the results with the Retinex algorithm to compensate the limitations of the tristimulus theory and to optimize the dynamic range of the typical display device. One of the problem, in the lighting model described is that material colors are characterized by the spectral reflectance, which is a tabulated function of wavelength, so surface appearance must be uniform. This was not a great problem for the materials constituting the Aosta Roman Theatre, travertine–ashlars and pudding stones, provided that they are observed at a distance that do not need to show their surface textures. We are working on

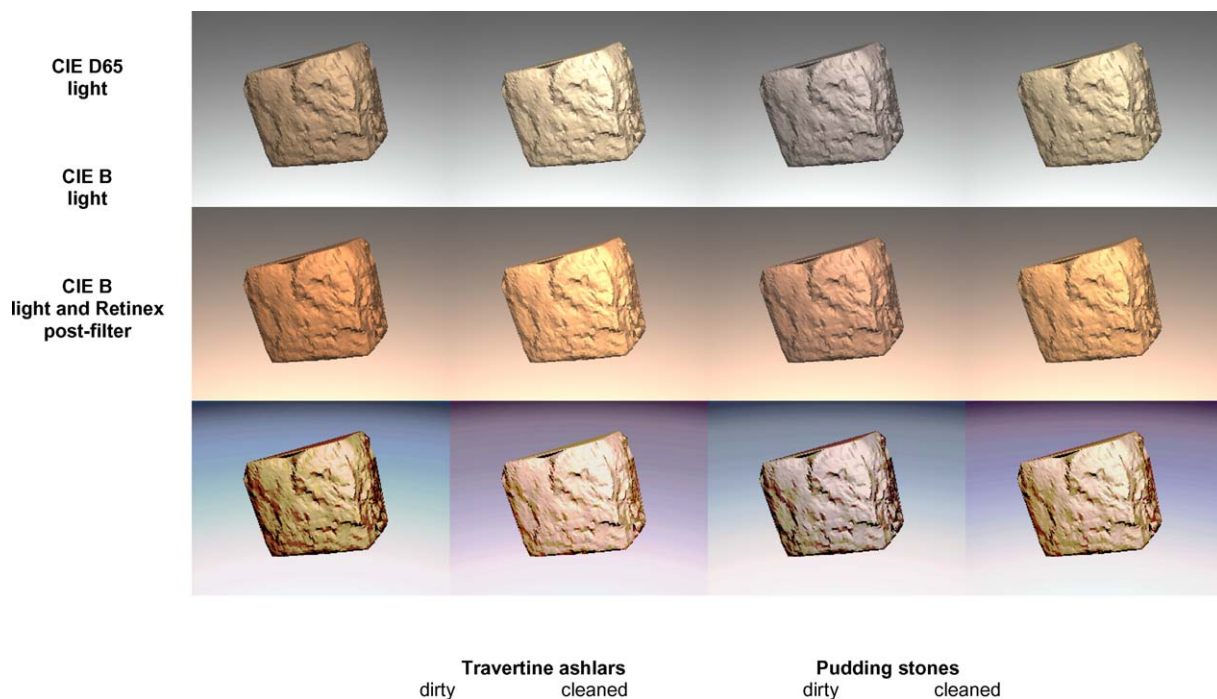


Fig. 12. Samples stones with different material, different cleaning condition and different light source. Spectrally computed, reduced to RGB values applying the tristimulus theory and post-filtered.

the problem of defining and measuring textures for materials defined on a spectral reflection basis.

Acknowledgements

This work is partially financed by the Italian CNR Project “Multimedialità : applicazione ai beni culturali”. Our greetings to L. Moltedo (IAC-CNR Roma), P. Salonia (ITABC-CNR Roma), O. Andrisano (University of Bologna CSITE-CNR), R. Picco (CST Torino), P. Fantucci (DCOMA, Università Milano), S. Tubaro (DEI, Politecnico di Milano), L. Appolonia (Sopr. BB.CC.AA., Aosta).

References

- [1] G. Wyszecki, W.S. Stiles, *Color Science: Concept and Methods, Quantitative Data and Formulae*, John Wiley & Sons, New York, 1982.
- [2] A.S. Glassner, *Principles of Digital Image Synthesis*, Morgan Kaufmann, New York, 1995.
- [3] D. Marini, A. Rizzi, A computational approach to color adaptation effects, *Image Vis. Comput.* 18 (13) (2000) 1005–1014.
- [4] D. Marini, A. Rizzi, M. Rossi, Color constancy measurement for synthetic image generation, *Journal of Electronic Imaging* 8 (4) (1999).
- [5] L. Moltedo, G. Mortelliti, O. Salvetti, D. Vitulano, Computer aided analysis of the buildings, *J. Cult. Herit.* 1 (1) (2000) 59–67.
- [6] G.C. Borgia, M. Camaiti, F. Cerri, P. Fantazzini, F. Piacenti, Study of water penetration in rock materials by nuclear magnetic resonance tomography: hydrophobic treatment effects, *J. Cult. Herit.* 1 (1) (2000) 127–132.
- [7] F. Pedersini, A. Sarti, S. Tubaro, Automatic monitoring and 3D reconstruction applied to cultural heritage, *J. Cult. Herit.* 1 (3) (2000) 301–313.
- [8] D. Marini, A. Canesi, C. Gatti, M. Rossi, Parallelising Accelerated Ray Tracing for High Quality Image Synthesis, *WTC94, Transputer Application and Systems '94*, IOS Press, London, 1994.
- [9] R.L. Cook, K.E. Torrance, A reflectance model for computer graphics, *Computer Graphics* 15 (3) (1981).
- [10] C.M. Goral, K.E. Torrance, D.P. Greenberg, B. Battaile, Modeling the interaction of light between diffuse surfaces, *Computer Graphics Proceeding Siggraph '84*, 1984.
- [11] IES Computer Committee, *IES Standard File Format for Electronic Transfer of Photometric Data and Related Information*, Technical report IES LM-63-1991, New York, 1991.
- [12] D. Marini, M. Rossi, L. Moltedo, O. Salvetti, *Virtual Reality And Web Tools To Convey The Visual Information Of Ancient Monuments*, *Computer Networks and ISDN System* 29 (1997) 1655–1660 Elsevier.
- [13] M. Guizzo, D. Marini, M. Rossi, P. Trapani, *Strumenti WEB per la sperimentazione di interventi di restauro di monumenti antichi*, *Conoscenza per Immagini '97*, ed, Il Rostro, Milano (1997) 49–56.
- [14] P. Salonia, A. Negri, G. Accardo, S. Scardigli, L. Appolonia, *Definizione di archivi di dati e immagini relativi ad analisi architettoniche dell'edilizia storica*, *Conoscenza per Immagini '97*, Il Rostro, Milano, 1997.
- [15] P. Salonia, A. Negri, *ARKIS: An Information System as a Tool for Analysis and Representing Heterogeneous Data on an Architectural Scale*, in: *Proceedings of the Conference in Central Europe on Computer Graphics, Visualization and Interactive Digital Media 2000, WSCG 2000*, University of West Bohemia Campus Bory, Plzen (Pilsen) Czech Republic, February 7–11, 2000.
- [16] F. Pedersini, S. Tubaro, *Accurate 3D Reconstruction from Trinocular Views through Integration of Improved Edge-Matching and Area-Matching Techniques*, *VIII EUSIPCO*, Trieste, 1993.
- [17] CIE, *Spatial Distribution of Daylight*, pub. CIE S003, 1996.
- [18] CIE, *Standard Illuminants for Colorimetry*, pub. CIE S005/ISO10526, 1999.
- [19] M. Rossi, A. Moretti, *Sintesi delle immagini per il fotorealismo*, Ed, Franco Angeli, Milano, 1998.
- [20] M. Rossi, D. Marini, A. Rizzi, *Photorealistic rendering over the Internet for restoration support of ancient buildings*, *Proceedings of the SPIE Electronic Imaging 2001—Internet Imaging II*, vol. 4311, San José California January 2001, pp. 226–235.
- [21] E. Land, J. McCann, *Lightness and Retinex Theory*, *J. Opt. Soc. Am.* A 61 (1) (1971) 1–11.
- [22] A. Rizzi, L. Rovati, D. Marini, F. Docchio, *Unsupervised Corrections of Unknown Chromatic Dominants using a Brownian Paths Based Retinex Algorithm*, *J. Electron. Imaging* July 2003; 12(3).
- [23] D. Marini, A. Rizzi, L. De Carli, “*Multiresolution retinex: comparison of algorithms*”, *First International Conference on Color in Graphics and Image Processing CGIP '2000*, Saint-Etienne, France, October 1–42000.
- [24] B. Funt, F. Ciurea, J.J. McCann, “*Tuning Retinex Parameters*”, *Proceedings of SPIE*, vol. 4662, *Human Vision and Electronic Imaging VII*, San Jose, January 2002.
- [25] S. Zeki, *A Vision of the Brain*, Blackwell Scientific Pub, Cambridge, 1993.